

# Sea glider navigation around a circle using distance measurements to a drifting acoustic source

Jan SLIWKA<sup>1,2</sup>, Benoît CLEMENT<sup>1,2</sup> and Irvin PROBST<sup>1,2</sup>

**Abstract**— This paper describes a simple yet robust sea-glider navigation method in a constellation of drifting Lagrangian drifters under the polar ice cape. The glider has to perform oceanographic measurements, mainly conductivity, temperature and depth, in the area enclosed by the drifters and can not rely on GNSS positioning data as the ice cape makes it impossible to surface. The originality of the presented method resides in the use of only one acoustic beacon and a very simple PID controller based on a basic kinematic model. Moreover, the method does not use a localization algorithm to estimate state space model data but interval analysis methods which allow to bound the errors. Validation is then performed through intensive simulations.

## I. INTRODUCTION

Deploying a constellation of drifting floating systems performing oceanographic measurements under the polar ice cape is part of the ACOBAR project (see [12]) as seen in Figure I.

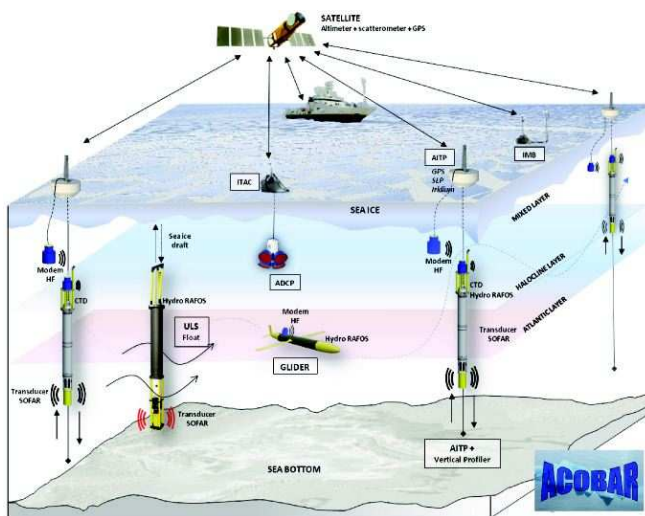


Fig. 1. ACOBAR project overview

In order to fill the gap in data between the Lagrangian drifters (denoted as "floats" from now on), a **sea-glider** has been chosen to navigate in between the floats. The floats are moored into the ice cape and used as acoustic beacons using RAFOS ([11]) emitters which sends a chirped acoustic signal at well known time slots. The frequency of this signal is usually in the 0-2 kHz interval, as the expected width

of the float network will be below 100 km, and as lower frequency emitters are very heavy and power consuming, the 1560 Hz RAFOS emitters are used here. Knowing the time of emission of several emitters, and measuring the time of arrival on a device one wishes to localize, is enough to get ranging measurements to each emitter and therefore localize the device in the emitters frame. On the other hand if one knows the position of several receiving devices it is possible to localize the emitters. Such low frequency signals can be detected at ranges up to 100 km for 1560 Hz, or even more for lower frequencies, but they can barely transmit any data.

The glider is supposed to navigate between the floats in order to collect oceanographic data, and once it gets close enough to a float (at most 10 km) a high frequency acoustic modem is used to download the data to the floats. Then the floats use their Iridium modem to relay these data to the operators.

The RAFOS localization has been proven to be efficient for decades but it puts a lot of constraints on the emitters network. Mainly there are two major issues:

- 1) The floats positions are to be known by the glider in order to compute its position, but the floats are drifting as the ice cape moves. As the glider can not surface to use satellite data networks the only way to transmit the floats positions is to use an acoustic link.
- 2) Usual localization methods, such as trilateration [9], require the glider to have at least three beacons in range, but once again the floats are moving and it is not possible to guarantee that the ice movements will not tear the float network apart.

One could think of using unary data coding between successive RAFOS emissions<sup>1</sup> to transmit data to the glider, this might solve the first issue but it will not prevent the network from getting too wide. Furthermore more issues are making real-time autonomous positioning an even more daunting task, for instance clock drifts, local variations in the speed of sound, and so on. Finally it is not possible to rely on a compass close to the magnetic pole, therefore even if the positioning problems could be solved the navigation would not be an easy task.

In order to solve these problems, this paper proposes a simple and robust navigation algorithm using the ranging data described above. Our approach is to split the localization of the glider, which is mandatory to geolocalize the oceanographic measurements, and the navigation task. The idea is

<sup>1</sup>ENSTA Bretagne / IT Department, 2 rue F. Verny, 29200 Brest, France  
firstname.name at ensta-bretagne.fr

<sup>2</sup> Lab-STICC UMR CNRS 6285

<sup>1</sup>For instance a 10 seconds delay between two successive RAFOS signals means a predefined variable has now the value "10".

to navigate around only one float, called the master float, and store the other floats' ranging data for post-processing once the data are transmitted to the operators. Doing this removes the need to know the glider position in real-time and gives the operators much more time and computing power to perform fine adjustments on the positioning data, therefore increasing the scientific value of the oceanographic measurements. Finally less tasks performed by the glider onboard software means a lower power consumption therefore longer missions.

The simplest motion possible around the master float is to follow a circular trajectory of a setpoint radius  $r$ . This radius can be changed during the mission in order to cover a wider area using unary coding as explained above. Since the trajectory is circular, the problem is invariant with rotation so the task can be performed using a gyroscope instead of a compass.

## II. NAVIGATION USING A SINGLE BEACON

Several authors considered navigation of AUVs using ranging data to a single beacon (see for example [3],[8] or [6]). This kind of navigation consists in the AUV (or beacon) localization in order to navigate around the beacon. But the main issue is that it is not possible to localize the beacon with only one measurement. The AUV has to make ranging measurements from different places while moving in order to perform the navigation. As a consequence the displacements of the AUV has to be known with maximal accuracy (using dead reckoning for example) in order to create a solid baseline for the trilateration. The AUV has to perform appropriate maneuvers to make the localization efficient. In [3], it is claimed that the trajectory which maximizes the information given by the measured ranges is when the vehicle describes a circle centered at the beacon.

In this article we propose a different approach which consists on using a simple regulator based on intuitive behavior. The regulator should be simple *i.e.* it includes no observation of the different unknown states of the problem. The method can be then validated using the viability theory [2] or using Monte Carlo testing methods (take several random initial conditions and make statistics on convergence).

The navigation algorithms are supposed to be:

- user friendly (few configuration parameters which tuning remain easy)
- robust to
  - variable and unknown perturbations (here sea current velocity and master float drift velocity)
  - measurement noises
  - missing or non regular measurements
  - outliers

## III. MOTION EQUATIONS

A sea glider is an AUV which moves without any propeller (see [15] or [4] for examples). ENSTA Bretagne has developed its own glider [10] and [5] presented in Figure III. Vehicle pitch and roll are controlled by two mobile masses and the buoyancy regulation is performed by a ballast. The glider cycle consists on:

- making it sinking while leaning down, until it reaches the desired depth
  - making it surfacing while leaning upwards.
- The yaw rate  $\omega$  is proportional to the roll  $\phi$ .



Fig. 2. ENSTA Bretagne Glider: Sterne

In this paper, only the 2D problem is considered where the ranging measurements are depth compensated. Moreover, the speed of the vehicle  $v_g$  is considered as a constant through time by neglecting the transitions during the gliding cycle. Figure 3 shows the different parameters which are used in the article.

### A. Notations

Denote by:

- $d$  the distance between the glider and the float
- $r$  the radius of the circle
- $\Delta r$  the width of the regulation zone
- $\psi$  the heading of the glider
- $v_g$  the velocity of the glider relative to water
- $\vec{v}_c$  the velocity vector of the relative current between the beacon and the glider ( $v_c = \|\vec{v}_c\|$  and  $\alpha = \arg(\vec{v}_c)$ ).

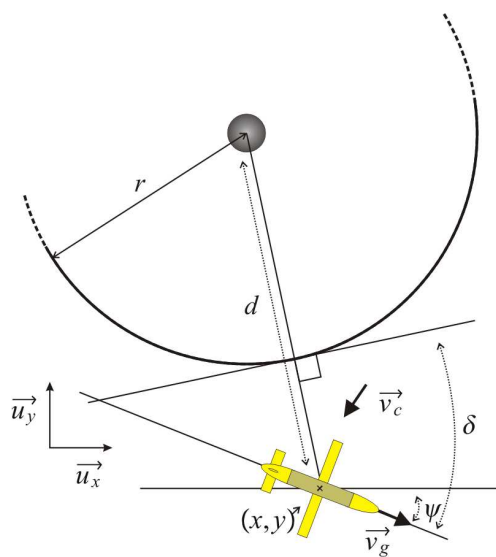


Fig. 3. The different parameters of the problem

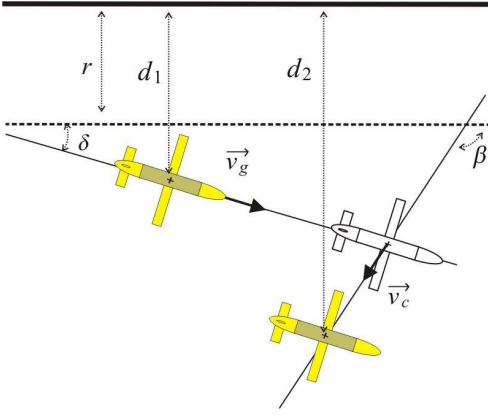


Fig. 4. Line following

- $\delta$  the angle between glider's heading and the tangent to the circle perpendicular to the line glider-Beacon.
- $\omega$  rotation speed of the glider

### B. Simulation oriented motion equations

For the simulation, we chose very simple equations to model the motion of the glider in the Cartesian workspace.

$$\begin{aligned} \dot{x} &= v_g \cos \psi + v_c \cos \alpha \\ \dot{y} &= v_g \sin \psi + v_c \sin \alpha \\ \dot{\psi} &= \omega. \end{aligned} \quad (1)$$

Note that these equations can be applied to other types of robots thus our navigation approach can be easily transposed.

### C. Regulation oriented motion equations

In order to obtain differential equations suitable for regulation, we consider the line following issue with range measurements to a reference line. Actually, this problem is equivalent to the circle following problem when the radius is big enough, indeed the trajectory will then be seen locally as a straight line. The Figure 4 shows an illustration of two consecutive glider states labeled, 1 and 2.

The new parameter  $\beta$  is the angle of the current relatively to the line to be followed.

We obtain the following state space model:

$$\begin{aligned} \dot{d} &= v_c \sin \beta + v_g \sin \delta \\ \dot{\delta} &= \omega \\ \dot{\psi} &= \omega. \end{aligned} \quad (2)$$

The main idea is to find a suitable regulator for this problem and apply it on the case of line following. In order to confirm this approximation we consider the reference frame formed by the line glider-beacon and the tangent to the circle which is perpendicular to it. Figure 5 shows an illustration of two consecutive glider states labeled 1 and 2.

By making a first order approximation, the following state space model is obtained:

$$\begin{aligned} \dot{d} &= v_c \sin \beta + v_g \sin \delta \\ \dot{\delta} &= \arctan \frac{v_c \cos \beta + v_g \cos \delta}{d} + \omega \\ \dot{\psi} &= \omega. \end{aligned} \quad (3)$$

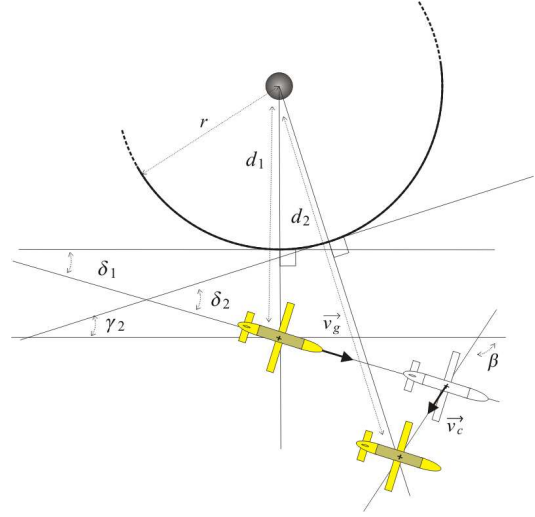


Fig. 5. The new parameters for the system glider - circle

The parameter  $\beta$  is the angle of the current with respect to the tangent of the circle perpendicular to the line glider-beacon. The current (since it is unknown) is considered as a time varying disruption. Note that when  $d \rightarrow \infty$  the state space equations become the same as in the case of line following. In that case, the line to be followed is the tangent to the circle.

## IV. REGULATION

In this part, the regulator is presented. It is designed to navigate on a circular trajectory of radius  $r$  around a float and to be robust to the initial conditions. Figure 6 shows the navigation strategy. We consider an area around the circle defined by a distance interval  $[r - \Delta r, r + \Delta r]$  where a PID regulator is used to maintain the desired trajectory. In this area, it is shown that the regulator is very efficient. Outside this interval, the strategy is to reach the reference circle using either *homing* or *escape* algorithms. In this article, we focus on the case of circle following. Even if the *homing* and *escape* issues are important, they remain out of the scope of this paper.

### A. PID controller

This section presents the controllers used to navigate on a circular trajectory. Due to discrete measurements, the discrete form of the controller is used.

It is possible to perform the circular navigation by making a control loop on either the heading  $\psi$  which can be measured using a magnetic compass for instance or on the yaw rate  $\omega = \dot{\psi}$ , which can be measured using a gyroscope.

Consider the error to be minimized:

$$e_k = \frac{d_k - r}{\Delta r} \quad (4)$$

where  $\Delta r$  defines the zone where the glider is regulated as seen on Figure 6.

We propose a PID controller for the yaw rate  $\omega$  in the classical form with  $K_1$ , the integral gain,  $K_2$  the proportional

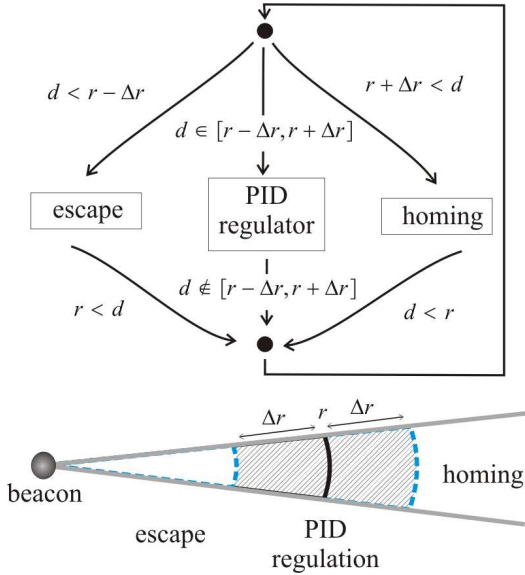


Fig. 6. Regulation diagram

gain and  $K_3$  the derivative gain. Note that only  $e$  is observed and the derivative term is to be estimated.

The glider makes range measurements every  $\Delta T$  time (here  $\Delta T$  is 20 minutes). Let consider the non recursive and recursive form (practical) of the discrete controller for the yaw rate:

$$\begin{aligned} I_{k+1} &= I_k + e_{k+1} \\ \omega_{k+1} &= K_1 I_{k+1} + K_2 e_{k+1} + K_3 \dot{e}_{k+1} \\ \omega_{k+1} &= \omega_k + K_1 e_{k+1} + K_2 (e_{k+1} - e_k) + K_3 (\dot{e}_{k+1} - \dot{e}_k) \end{aligned} \quad (5)$$

where  $\dot{e}_k$  is the estimate of the derivative at time step  $k$ . As an example, when the data is not noisy one can take the first order approximation:

$$\dot{e}_k = \frac{(e_{k+1} - e_k)}{\Delta T} \quad (6)$$

By considering the following approximation

$$\omega_{k+1} = \frac{\psi_{k+1} - \psi_k}{\Delta T} \quad (7)$$

the recursive form for the yaw controller can be derived from the formula for the yaw rate controller:

$$\psi_{k+1} = \psi_k + \Delta T (K_1 I_{k+1} + K_2 e_{k+1} + K_3 \dot{e}_{k+1}) \quad (8)$$

The non recursive formula can be easily derived from the recursive one.

Close to the magnetic pole, compasses are not working properly. It would be logical to use a gyroscope to perform this regulation but due to very slow dynamics of the system (sample time is more than 20 minutes) this is not possible without a very precise gyroscope. Then another strategy has to be defined. The proposed solution is to use the recursive control formulation for the heading:

- make heading corrections (which takes little time: less than a minute) using a gyroscope;
- switch on a open loop mode assuming the glider will move in a straight line. This is true in the fluid frame since the glider is designed in this way (if  $\phi = 0$ ).

As a consequence, in both gyroscope or compass based navigation, the yaw controller recursive formula (8) is used.

Note that the integral term is not necessary to have a descent trajectory (see Simulation results) unless one wants a perfect circle. Therefore the integral term can be discarded. Besides it is an additional constant to fix and there is a need for anti wind-up strategies which adds some additional constraints. In this paper, the *keep it simple first* approach leads to choose  $K_1 = 0$ .

## V. NOISE AND OUTLIERS REJECTION

The measurements are subject to Gaussian white noise with a standard deviation of  $\sigma$ . The problem of the noise is that it makes it difficult to estimate the derivatives necessary for navigation. Furthermore, there the measurements are corrupted with outliers often due to abnormal propagation of the acoustic signal such as multiple paths trajectories. The proposed algorithm takes into account both noises and outliers. The main idea is to use robust linear regression on the data. The proposed algorithm uses set membership methods which consider sets of possible values instead of probability distributions in a stochastic approach.

### A. Robust regression

Consider  $n$  measurements of an unknown variable  $y$  at different times  $t_k$  denoted  $\tilde{y}(t_k)$ ,  $k \in \{1, \dots, n\}$ . The measurements are subject to noise which we consider contained in an interval  $[-\varepsilon, \varepsilon]$ . We consider that  $\tilde{y}(t_k)$  is not an outliers if

$$\exists w \in [-\varepsilon, \varepsilon], \tilde{y}(t_k) = y(t_k) + w \quad (9)$$

The possible values of  $y(t_k)$  belong to an interval denoted  $[y_k]$  defined as follows

$$y(t_k) \in [\tilde{y}(t_k) - \varepsilon, \tilde{y}(t_k) + \varepsilon] = [y_k] \quad (10)$$

The idea behind set membership linear regression is to find the set of all possible lines which pass through all possible values of  $y(t_k)$ ,  $k \in \{1, \dots, n\}$ . If there are no outliers, this consists on finding the set of parameters  $(a, b) \in \mathbb{R}^2$  which satisfy the following equations

$$\begin{aligned} C_k : a * (t_k - t_n) + b &= y_k, \\ y_k &\in [y_k], \\ (a, b) &\in \mathbb{R}^2, k \in \{1, \dots, n\}. \end{aligned} \quad (11)$$

This formulation of the problem corresponds to a continuous CSP (Constraint Satisfaction Problem) described in [1]. A CSP is defined by:

- a set of equations (also called constraints) here denoted  $C_1, \dots, C_n$ ,
- a vector of all the variables involved in the problem  $(a, b, y_1, t_1, \dots, y_n, t_n)$ ,
- the domains of those different variables.

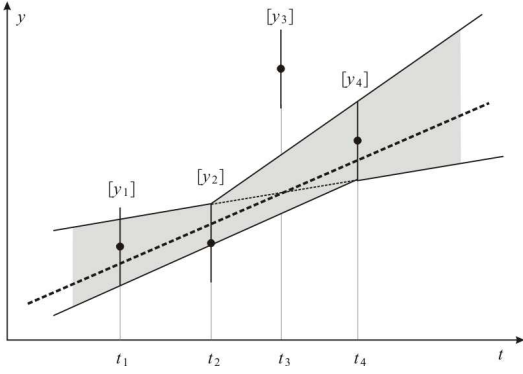


Fig. 7. Example of robust linear regression

Solving a CSP consists on finding the parameters  $(a, b) \in \mathbb{R}^2$  satisfying all the constraints. In case of outliers, this CSP does not admit any solution. Therefore, we search for the parameters  $(a, b) \in \mathbb{R}^2$  satisfying most of the constraints. This approach was considered in [13], [14] and [7].

Figure 7 shows the envelop (in gray) of all the lines consistent with a maximum of measurements (here 3) in a simple example involving 4 measurements with one outlier. The outlier is detected and rejected. The hyphened represents the real line in the example.

The CSP solvers returns a set of possible values of the parameters  $(a, b) \in \mathbb{R}^2$ . We usually take the center of gravity of that set as a punctual representative. Note that the CSP solvers are not limited to linear equations. It is possible to use all kind of non linear equations such as higher order polynomials or trigonometric functions. We used a linear model for its simplicity.

### B. Correcting range measurements

Consider the last (non missing)  $n$  measurements measured with an error in  $[-\varepsilon, \varepsilon]$  at the time steps  $t_1, \dots, t_n$ . If the trajectory was a line, one could apply the robust regression directly on those measurements (which also evolve linearity) to compute the coefficients of the best fit line  $a$  and  $b$  as explained in the previous subsection. The coefficient  $b$  corresponds to the current corrected range measurement. The coefficient  $a$  corresponds to an estimate of the derivative of  $d$  i.e. the derivative of the error used in the PID controller.

Due to the glider regulation, the trajectory is not a line but a sequence of lines. In order to apply the robust regression, we have to transform this sequence into a straight line or a set of parallel lines named a corridor as shown in Figure 8. The width of the corridor is denoted  $\varepsilon_d$  and is to be calculated. This value  $\varepsilon_d$  is then added to the range measurement error which becomes  $[-(\varepsilon + \varepsilon_d), \varepsilon + \varepsilon_d]$  and the robust linear regression algorithm can be applied.

The real range values are unknown but their variation is given by the state space equations in (2). In order to determine  $\varepsilon_d$  we use the following state equations focusing on evolving terms of the glider state equations. We assume

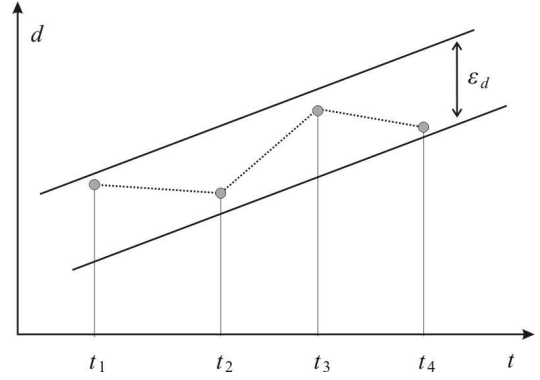


Fig. 8. Fitting the local trajectory in a corridor

$\beta$  is constant due to slow dynamics of the problem:

$$\begin{aligned} \dot{x} &= v_g \sin y \\ \dot{y} &= u \end{aligned} \quad (12)$$

Note that the input  $u$  is perfectly known. Then for each initial condition  $(x, y)$ , it is possible to compute a linear corridor of width  $\varepsilon_d(x, y)$  enclosing the points  $(x_k, t_k), k \in \{1, \dots, n\}$ . These last points are computed by simulation of the state space model (12) and  $\varepsilon_d(x, y)$  is calculated as follows:

- compute the linear regression
- the greatest and the least distances between the points and the line determine the width of the corridor  $\varepsilon_d(x, y)$

The initial condition on  $x$  doesn't affect the computations of  $\varepsilon_d(x, y)$ .

Let us consider the following definition of  $\varepsilon_d$ :

$$\varepsilon_d = \max(\varepsilon_d(0, y), y \in \left[-\frac{\pi}{2}, \frac{\pi}{2}\right]). \quad (13)$$

Note that most of the time, the max value is obtained for small  $y$  ( $\delta = 0$  maximizes the variations of the acceleration of  $d$ ).

## VI. SIMULATION RESULTS

Figure 9 shows simulation results for the following parameters:

$$\begin{aligned} v_g &= 0.3m/s, v_c = 0.15m/s, \alpha = -\frac{\pi}{2} \\ r &= 10km, \Delta r = 3km, \\ \varepsilon &= 150m, outliers = 10\%, missing = 10\% \\ K_1 &= 0, K_2 = 0.2, K_3 = 0.6, n = 6 \end{aligned} \quad (14)$$

The gray lines are the measurements, the black dots are the trajectory.

In order to increase the area where the glider makes measurements, the glider can follow a helicoidal trajectory as shown in Figure 10. The outliers and the missing data can clearly be seen on the image. In the presented simulation, the glider performs an helicoidal trajectory starting at 20 km and ending at 5 km with a step of 3 km.

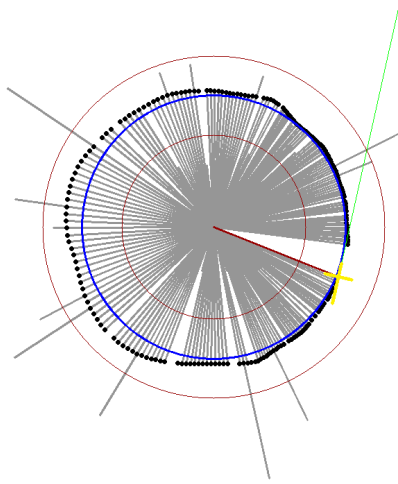


Fig. 9. Result of regulation

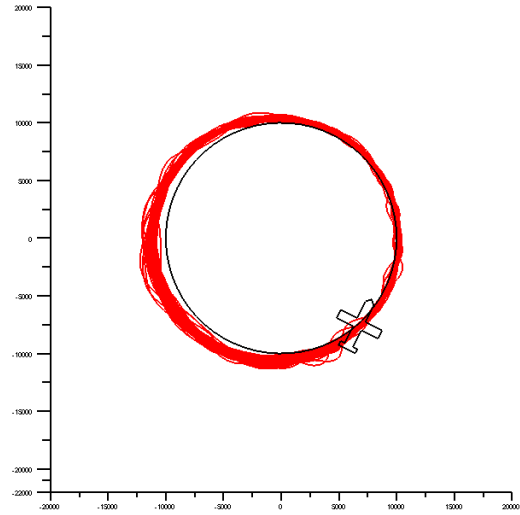


Fig. 11. One year navigation (distances are in meters)

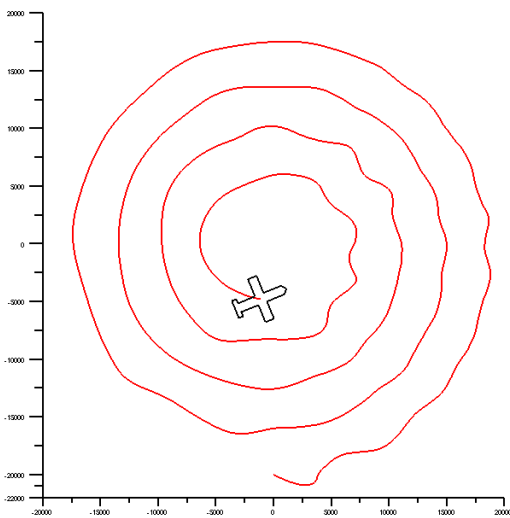


Fig. 10. Using a helicoidal trajectory to cover a wide area (distances are in meters)

## VII. VALIDATION

Validation is performed with simulations; the Figure 11 shows the trajectory of the robot for a duration of one year around a circle of 10 km radius. Not even once the robot has quit the circle area.

## VIII. CONCLUSION

As for now, the main point is that this algorithm satisfies the requirements and it remains very simple. The algorithm can be improved using more advanced techniques such as a better regulator than a PID. The best tuning can be found through simulations and should be good approximations for the real glider. The algorithm can be validated using methods described in II. Finally, many assumptions have been made concerning the nature of the data (noise evolution with

distance, outliers rate, missing data rate...) which are to be confirmed through experiments.

## REFERENCES

- [1] Krzysztof R. Apt. *Principles of Constraint Programming*. Cambridge University Press, 2003.
- [2] J.P. Aubin. *Viability Theory*. Boston-Birkhauser, 1991.
- [3] P. Baccou and B. Jouvencel. Homing and navigation using one transponder for auv, postprocessing comparisons results with long base-line navigation. In *Robotics and Automation, 2002. Proceedings. ICRA '02. IEEE International Conference on*, volume 4, pages 4004 – 4009 vol.4, 2002.
- [4] C.C. Eriksen, T.J. Osse, R.D. Light, T. Wen, T.W. Lehman, P.L. Sabin, J.W. Ballard, and A.M. Chiodi. Seaglider: a long-range autonomous underwater vehicle for oceanographic research. *Oceanic Engineering, IEEE Journal of*, 26(4):424 –436, oct 2001.
- [5] Floc'h F. *Prédiction de trajectoires d'objets immergés par couplage entre modèles d'écoulement et équations d'Euler-Newton*. PhD thesis, ENSTA-Bretagne and UBO, France, 2011.
- [6] B. Ferreira, A. Matos, and N. Cruz. Single beacon navigation: Localization and control of the mares auv. In *OCEANS 2010*, pages 1 –9, sept. 2010.
- [7] L. Jaulin. Robust set membership state estimation ; application to underwater robotics. *Automatica*, 45(1):202–206, 2009.
- [8] M.B. Larsen. Synthetic long baseline navigation of underwater vehicles. In *OCEANS 2000 MTS/IEEE Conference and Exhibition*, volume 3, pages 2043 –2050 vol.3, 2000.
- [9] D.E. Manolakis. Efficient solution and performance analysis of 3-d position estimation by trilateration. *IEEE transactions on Aerospace and Electronic Systems*, 32:1239–1248, 1996.
- [10] R. Moitie and N. Seube. Guidance and control of an autonomous underwater glider. In *Proceedings of 12th Int. Symposium on Unmanned Untethered Submersible*, Durham, NH, USA, 2001.
- [11] T. Rossby, D. Dorson, and J. Fontaine. The rafos system. *Journal of atmospheric and oceanic technology*, 3:672–680, 1986.
- [12] Stein Sandven. ACOBAR - acoustic technology for observing the interior of the arctic ocean. <http://acobar.nersc.no>, 2009.
- [13] J. Sliwka. *Using set membership methods for robust underwater robot localization*. PhD thesis, ENSTA-Bretagne and UBO, France, 2011.
- [14] J. Sliwka, F. Le Bars, O. Reynet, and L. Jaulin. Using interval methods in the context of robust localization of underwater robots. In *NAFIPS11*, El Paso, Texas, 2011.
- [15] D.C. Webb, P.J. Simonetti, and C.P. Jones. Slocum: an underwater glider propelled by environmental energy. *Oceanic Engineering, IEEE Journal of*, 26(4):447 –452, oct 2001.